ESTUARINE WETLAND HABITAT TRANSITION INDUCED BY RELATIVE SEA-LEVEL RISE ON MUSTANG AND NORTH PADRE ISLANDS, TEXAS: PHASE I

James C. Gibeaut, Ph.D.

Eleonor Barraza, M.S.

Boris Radosavljevic, B.S.

Coastal and Marine Geospatial Laboratory
Harte Research Institute
Texas A&M University – Corpus Christi

6300 Ocean Drive
Corpus Christi, Texas 78412-5869
Voice: 361-825-2020
Fax: 361-825-2050
James.gibeaut@tamucc.edu

July 2010

Table of Contents

List of Figures

Acronyms

ALTM – Airborne Laser Terrain Mapper

DEM – Digital Elevation Model

IPCC – Intergovernmental Panel on Climate Change

kts – nautical miles per hour

Lidar – Light detection and ranging

m - meters

MHHW – Mean Higher High Water

mm/yr – millimeters per year

NOAA – National Oceanographic Atmospheric Administration

SLR – Sea-Level Rise

USGS – United States Geological Survey

Introduction

From 1948 to 2006, sea level rose about 30 cm relative to the land (relative sea-level rise) in the Texas Coastal Bend as measured by the Rockport tide gauge (NOAA, sea level trends website, http://tidesandcurrents.noaa.gov/sltrends/sltrends.shtml). It is clear that this rise has caused changes in the distribution of wetlands and is partially responsible for wetland loss through inundation (Gibeaut et al, 2003; White et al., 2006). Climate change models predict that the rate of global sea-level rise will increase over the next decades (IPCC, 2001), but even if the predicted increase does not occur, we can still expect a rise of about 50 cm over the next 100 years based on projecting the 58-year Rockport record into the future. This amount of rise is large considering a tide range of 20 cm or less, low-lying and gently sloping barrier islands and coastal plains, and increasing human use of the central Texas coast.

White et al. (2006) measured estuarine tidal flat loss of 57% (3,974 ha to 1,695 ha) on Mustang Island from the 1950s to 2002-04. During the same time period, seagrass and marsh and mangrove gained in area as low flats were flooded and changed to open water or seagrass areas and higher flats converted to marsh. White et al. (2006) also documented a gain in low marsh from 1979 to 2002-04 from 153 to 501 ha and a decline in high marsh during the same period. They also documented marshes migrating into upland areas, partially offsetting losses. The conversion of uplands to wetlands is an important process to sustain wetland environments during sea-level rise (Brinson et al., 1995), especially where vertical and horizontal accretion is not sufficient to stem drowning or edge erosion. Wetlands will not be able to migrate into uplands, however, if the slopes are too steep or structures, such as buildings or seawalls, prevent it. This means that even if we prudently plan barrier island development for today's environmental conditions, those plans may be inadequate for future conditions. Therefore, a way to predict change is needed to better manage for the future environment today, and this is the impetus for the work described herein. Map results from the model will be used in a geohazards map for the area during phase II of this project.

Quantitative marsh sedimentation models have been used to simulate the vertical development and maintenance of tidal flat/marshes at discrete locations (Allen, 1990;

Callaway et al., 1996; Krone, 1987; Temmerman et al., 2003). These models are tools for gaining a better understanding of the relative importance of mineral and organic sedimentation, compaction, tidal elevations, and sea-level change in the vertical accretion of tidal flats/marshes. They do not, however, describe how flats and marshes will transition across a landscape under the influence of sea-level change. This report presents such a model that provides maps and statistics estimating future wetland distributions based on assumptions of continued relative sea-level rise. The central concept of the model is that the distribution of wetland types is strongly dependent on elevation relative to mean high water and, as the level of mean high water changes, wetlands will shift horizontally to stay within their elevation range. The model was developed for and applied to Mustang Island and the northern part of North Padre Island in the Corpus Christi Bay system (Figure 1). Map results from the model will be used in a geohazards map for the area during phase II of this project.

Barrier Island Wetlands and Sea-Level Rise

Barrier island habitat types and the effects of geological and biological processes are closely tied to height relative to sea level (Gibeaut et al., 2003). The style of transition of estuarine wetland habitats during rising sea level depends largely on the slope of the upland and sediment supply (Brinson et al., 1995). Fringing wetlands on the barrier islands of Corpus Christi Bay exist within a narrow elevation range, with shifts from barren tidal flat to marsh to upland vegetation occurring across areas with just a 50- to 60-cm rise in elevation. On the bay side of Mustang Island, this amount of topographic change occurs on horizontal scales of a few 10's of meters and in complicated patterns across relict geomorphic features, such as storm-surge channels, dunes, deflation flats, and washover and flood-tidal delta deposits.

Inundation by the sea is not the only process that causes shifts in the patterns of wetlands. Erosion or accretion along the shoreline caused by waves and tidal currents may be significant in some areas, and vertical accretion of wetland surfaces, through both mineral sediment deposition and organic matter production, may offset the effects of sea-level rise. Land subsidence and sediment compaction, on the other hand, effectively increase the rate of sea-level rise.

6
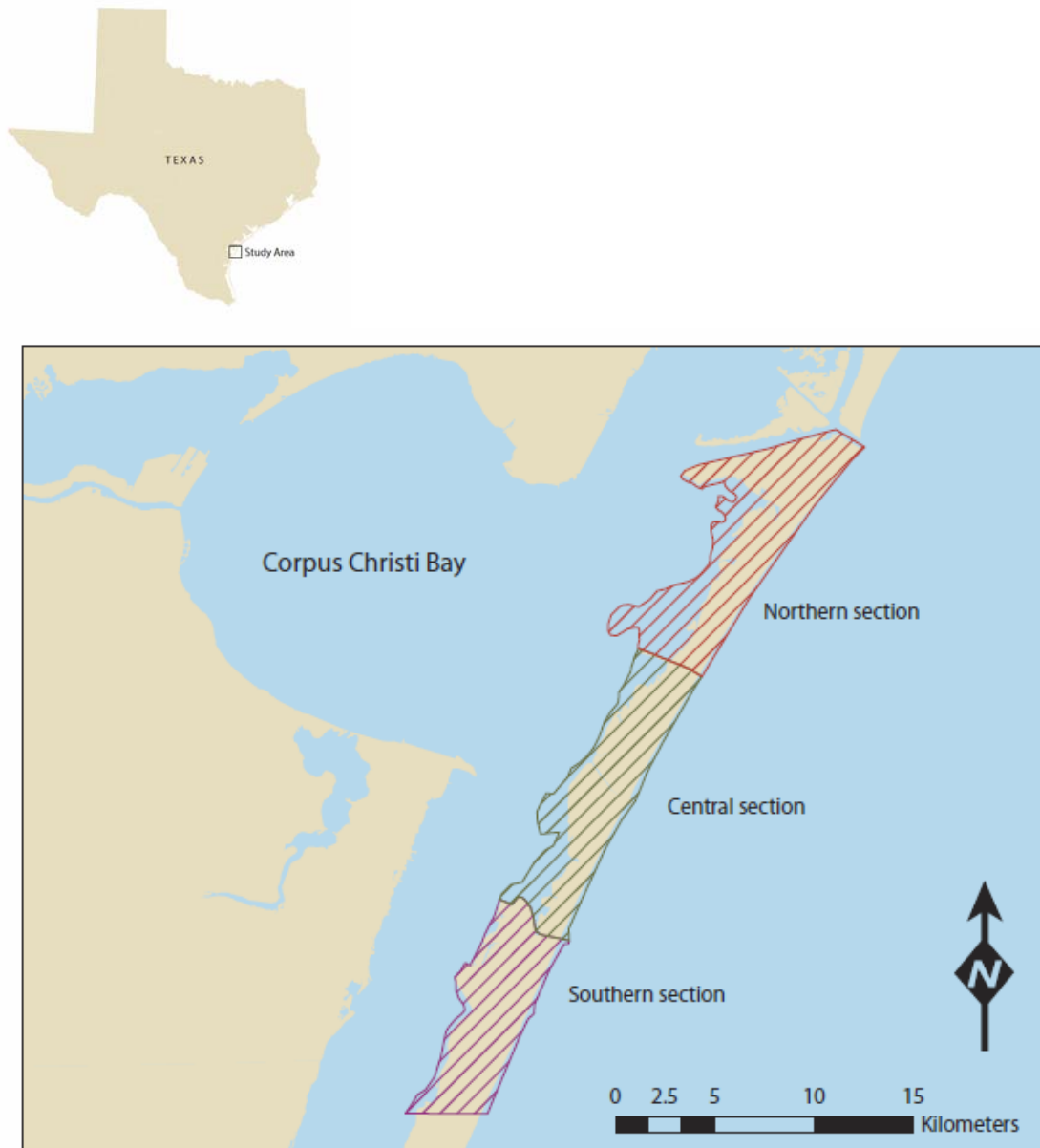
Figure 1. Study areas on Mustang and North Padre Islands. The sections are how the area was divided for model runs.

Modeling Approach

The modeling approach relies on the association of estuarine wetland habitat types and elevation. First we quantify the topographic relationships of habitat types so that we can classify a study area as different habitats using a Digital Elevation Model (DEM). In one-year steps, the DEM is raised or lowered to simulate sea-level change.

The model also adjusts the DEM to simulate land subsidence, vertical accretion caused by sediment deposition, and the retreat and advance of the shoreline (Figure 2). The resulting DEM is reclassified into habitat types. The following sections describe the components of the model that have been applied to the study area.
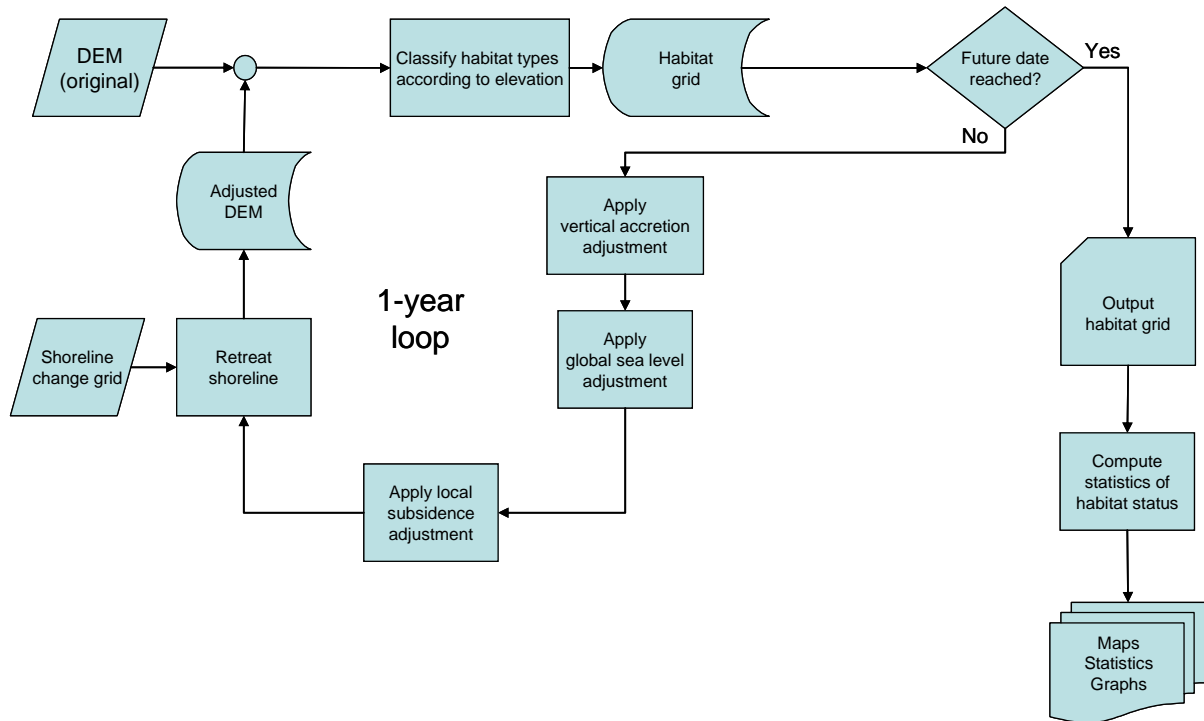
Figure 2. Flow diagram for modeling wetland habitat transition during sea-level change.

Lidar-derived Digital Elevation Model (DEM)

A highly detailed and accurate topographic model is required to show the subtle and complicated patterns of coastal habitats that are controlled by topography on barrier islands. Before the advent of scanning airborne topographic lidar technology in the mid 1990's, however, topographic models sufficient to form the basis of habitat transition models like the one presented here were not available. Lidar-derived DEMs with 1-m data postings and 10 to 20 cm vertical accuracy are required for realistic sea-level rise modeling of micro tidal barrier island wetlands such as Mustang Island (Gibeaut et al., 2003).

During the summer of 2005, the Bureau of Economic Geology of the University of Texas at Austin acquired topographic lidar data of the study area. The lidar survey was flown at a speed of about 100 kts and at a height 500 to 800 m above the ground with at

least a 60 percent overlap between flight lines. The Optech model ALTM 1225 lidar instrument was set at a 25 kHz pulse repetition rate. The aircraft stayed within 30 km of a GPS base station, and a ground calibration target was surveyed during each flight. These survey parameters provided an average data point spacing of closer than 1 m. The last return lidar data points were processed into 1-m DEMs, which have a vertical accuracy of about 10 cm on non-vegetated surfaces.

For this project, the DEMs were processed to remove features that could affect modeling results. Algorithms were developed and applied to the DEM to filter water surfaces, buildings, and relatively tall vegetation, particularly mangrove. Ideally, the DEM would represent the elevation of the substrate beneath vegetation cover, but lidar technology has limitations in this regard. Vegetation typical of the estuarine wetlands and back barrier uplands in the study area causes a vertical bias and added noise in the elevation data because of laser reflections from within the vegetation canopy. This vegetation effect proved to be troublesome in the Black Mangrove areas on Mustang Island.

Figure 3 is a ground-surveyed transect of the substrate on Matagorda Island, a barrier island north of the study area, with lidar data points and vegetation height superimposed. The lidar data points fall within the vegetation canopy but 0.1 to 0.2 m above the substrate in the low marsh, which is dominated by very dense *Batis maritima*. The upland area included low mesquite trees and *Spartina spartinae*, and some lidar data points reflected from tree tops. Upland and wetland areas on Mustang Island are mostly void of trees and bushes higher than 2 m, but scattered clumps do occur and these areas were removed from the lidar data using a newly developed algorithm. Wetland vegetation on Mustang Island, other than mangrove areas, is dominated by plants less than 0.5 m high and generally less dense than the *Batis maritima* along the Matagorda transect. Therefore, the effect of vegetation on the lidar DEM used in our model is probably less than that shown for the transect in Figure 3. No attempt was made to remove the effects of low vegetation from the model DEMs.
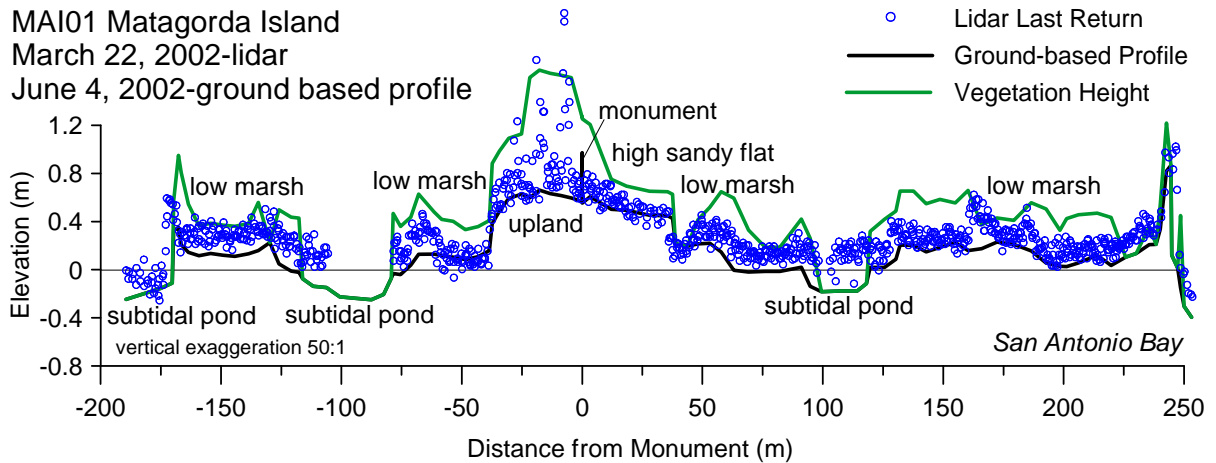
Figure 3. Lidar data points compared to ground survey of substrate and vegetation height. Selected lidar data points fall within 1 m of the transect line. Transect is on Matagorda Island, Texas in an area with dense estuarine wetland vegetation (primarily *Batis maritima*) (from {Gibeaut et al., 2003}.

Topographic Habitat Classification

Earlier produced wetland maps were combined with the DEM to determine elevation intervals for classifying the DEM into habitats. White et al. (2006) used 2002-2004 color infrared aerial photography and field checks to manually map wetland environments on Mustang and North Padre Islands according to the classification system of Cowardin et al. (1979). The aerial photographs were digital images with a pixel resolution of 1 m and registered to USGS Digital Orthophoto Quadrangles. Wetlands were mapped on computer screens at a scale of 1:4,000. For this project, the wetland map was field checked and classification discrepancies resolved. The wetland map data were also more accurately georeferenced using the DEM and more recent photography as control (Figure 4).

Elevation dependence of wetland type varies in the study area because of spatial variance in tide range and wave exposure. For this reason, elevation intervals used to classify each cell of the DEM were calculated for each cell. To accomplish this the polygonal wetlands map was rasterized into a grid with 1-m cells with the same coordinates as the 1-m DEM. For each wetland type, two new grids were computed. The values of one grid are the mean elevations of a particular wetland type in a 2 km by 2 km window surrounding the cell. The other grid holds the standard deviations of elevations of the surrounding wetland type from the same window. During each one-year model step, the DEM is classified into 5 categories: low flat; low marsh; high flat; high marsh;

10

and upland. For each cell in the input DEM, the mean and standard deviation grids for each wetland type are consulted to determine the most likely wetland type to assign to that particular cell. If the elevation is higher than the highest wetland type plus one standard deviation for that particular cell, then the cell is classified as upland.
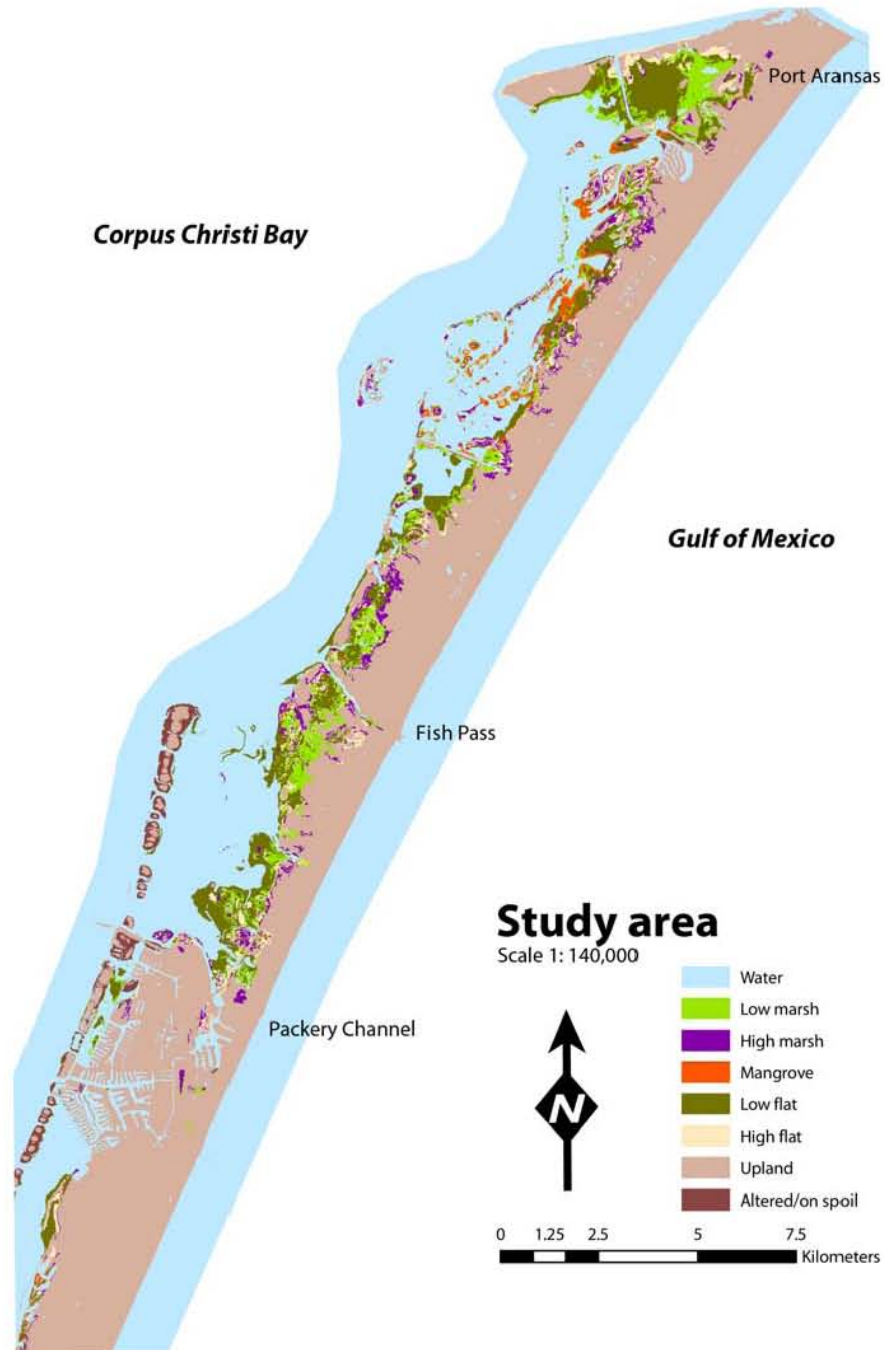
Figure 4. Simplified estuarine wetlands map as adjusted from 2002-2004 map data of White et al. (2006).

Elevation is the primary factor in determining estuarine habitat environments, but not the only factor, therefore, there are differences in the mapped and DEM classifications. Proximity to open bay waters and tidal creeks may also control the development of low or high marsh, flats or uplands. The effect of vegetation on the precision of the DEM also decreases the consistency of the classification. Furthermore, the relatively small mapping scale of the manually drawn habitat map compared to the 1-m DEM classification scale causes differences although the DEM classification may do a better job breaking out habitats that were combined in the manual mapping. Even with the differences between the mapped and DEM-classified habitat designations, the resulting classified DEMs appear realistic and true to the overall patterns of habitat distribution.

Vertical Accretion

Vertical sediment accretion occurs and partly offsets the inundating effects of relative sea-level rise. A sedimentation model for vertical accretion, therefore, is included in the habitat transition model (Figure 5). The sedimentation model is consistent with measured accretion rates and calculated hydroperiods. Twenty short cores were acquired from the study area and analyzed for sedimentological properties and for the Cesium-137 isotope. Cesium-137 is a product of atmospheric nuclear bomb testing conducted in the 1960's before the Limited Nuclear Test Ban Treaty went into effect. A peak in atmospheric fallout occurred in 1963 and elevated levels of Cesium-137 in sediment layers provide a time horizon of 1963. Using this time horizon, vertical accretion rate may be determined for the last 47 years.

Similar to vertical accretion rate studies along the upper Texas coast (e.g., Callaway et al. (1997), we measured lower vertical accretion rates at higher elevations. At the upland-wetland boundary, accretion rates measured in the cores approach zero and in low-marsh settings rates approach the long-term rate of relative sea-level rise of 5.2 mm/yr. This trend of higher accretion rates in lower elevations is caused by the longer duration (hydroperiod) and depth of inundation that brings more sediment to an area and allows it to be deposited during tidal cycles (Temmerman et al., 2003). Core analyses also show mineral sedimentation dominates, while the organic faction typically accounts for only a few percent of the sediment volume.

The vertical accretion model determines accretion as a function of elevation and is consistent with core analyses. The highest accretion rate is set at the lower low-marsh boundary and equals the rate of relative sea-level rise calculated using a linear regression for water levels measured from 1948 through 2006 (5.2 mm/yr) at the Rockport tide gauge. Once a marsh converts to open water, the model assumes it can not accrete to become emergent. A cell that converts to water during the model run can only become emergent wetland if sea level drops sufficiently. Below the low-marsh boundary, therefore, the vertical accretion rate is set to zero, and above the boundary, accretion rate decreases according to the expected duration of tidal inundation calculated using a sine wave function. At and above the high-marsh-upland boundary, the vertical accretion rate is zero. A different vertical accretion function is applied to each DEM cell because of differences in the elevations of the habitat boundaries used to constrain the model.
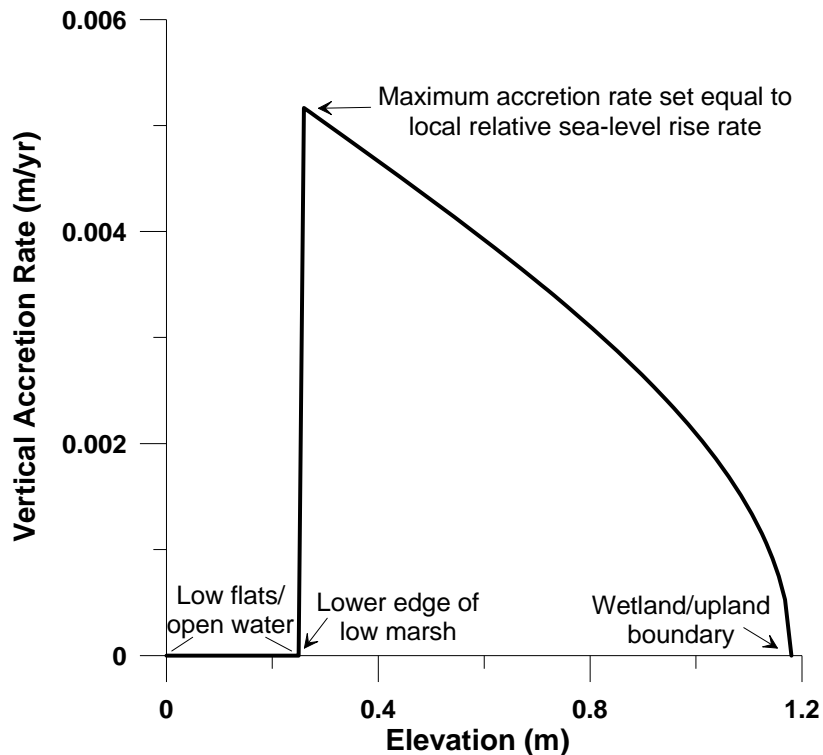
Figure 5. Vertical accretion function for a cell with an upland boundary elevation of 1.18 m and a low-marsh lower boundary of 0.25 m. The function is adjusted for each cell in the model according to the specific elevation of the low marsh and upland boundaries for that cell.

Relative Sea-Level Change

The actual water level record recorded by the Pier 21 tide gauge on the bay side of Galveston Island was modified to serve as input to the habitat transition model. This tide gauge has recorded a 96-year record of relative sea level change, and the mean sea level trend from 1908 to 1999 was a rise of 6.5 mm/yr (Zervas, 2001) . The Rockport gauge is closer to the study area, but its record only goes back to 1948 and there is a gap from 1955 to 1963. The Rockport record is long and complete enough, however, to calculate a long-term sea-level rise rate of 5.2 mm/yr and the decadal scale variation in water level is similar to the Pier 21 record. The Pier 21 record, therefore, was adjusted to have a long-term linear trend equal to the Rockport location, and this time series was used as input to the model. About 2- to 3-mm/yr of the Rockport sea-level rise rate is caused by local land subsidence. This amount of subsidence appears to be and is assumed to be representative of the study area and is included as input to the model.

Figure 6 shows a 3-year moving average of the water-level record for mean higher high water (MHHW), which is the tide level most significant in determining the elevation of the wetland/upland boundary. Superimposed on the rising trend are decadal-scale variations with amplitudes of 0.1 to 0.2 m. We expect there is a lag time for habitats to adjust to water level changes, therefore, to generate the time series to drive the habitat transition model, we use a 3-year moving average so that each year is the average of that year and the 2 previous years. Figure 7 shows the annual rate of MHHW change which is the derivative of the 3-year moving average in Figure 6 and is the time series that is input into the model.

Shoreline Change

In addition to changes caused by inundation, wetlands in the study area erode along the bayward fringes as a result of waves and tidal currents. Historic shorelines were compared from the 1930's, 1950's, 1982, 1995, and 2005. The 2005 shoreline was mapped during this project using the DEM while the earlier shorelines were mapped by researchers at the Bureau of Economic Geology at The University of Texas at Austin for prior studies. The shoreline configurations are very complicated and making reasonable projections for future shoreline movement in direction and magnitude based on past

14

shoreline change turned out not to be reasonable. Shoreline change in the model, therefore, only results from inundation.
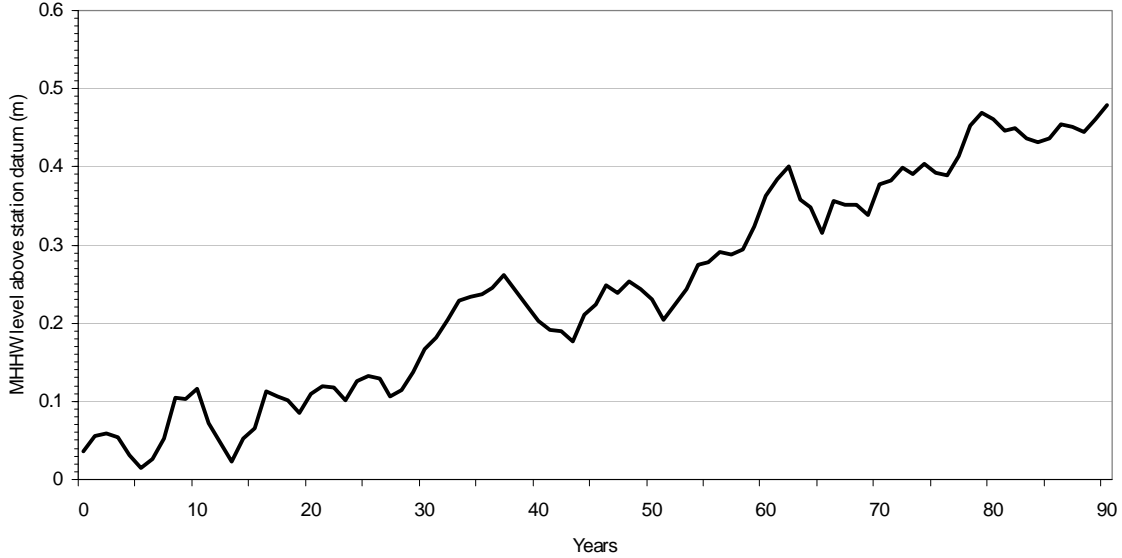
Figure 6. Adjusted three-year moving average of mean higher high water (MHHW) measured by the Pier 21 tide gauge on the bay side of Galveston Island. This original time series started in 1908 and has been adjusted to have a linear trend equal to the Rockport tide gauge (5.2 mm/yr). The 3-year moving average is the average of the current year, based on hourly water level measurements, and 2 previous years.
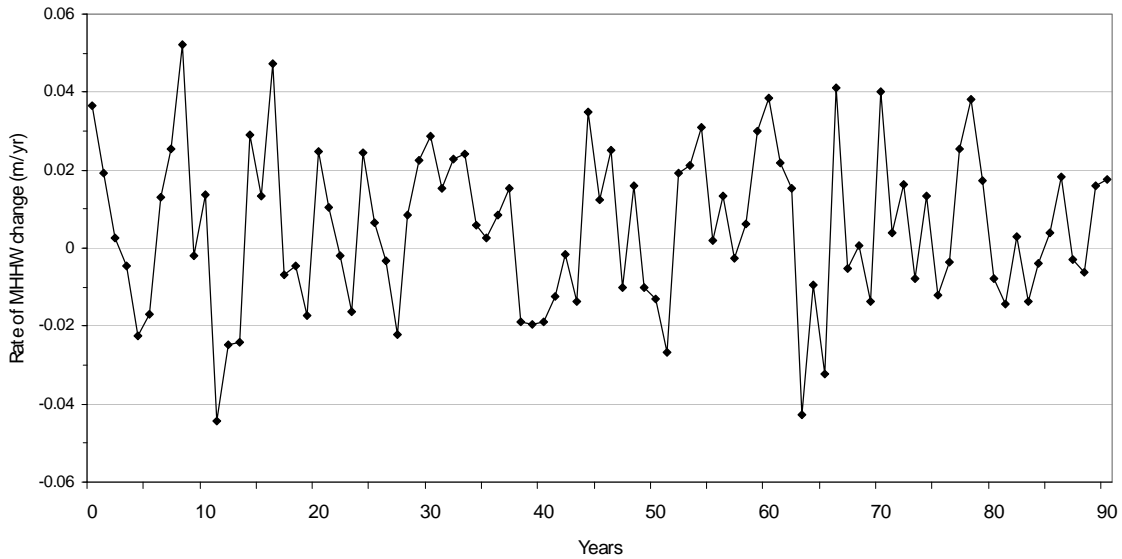
Figure 7. Year-to-year rate of change in mean higher high water (MHHW) computed from the 3-year moving average of MHHW change (Figure 6). This time series drives the habitat transition model.

Model Execution

The habitat transition model is implemented in a FORTRAN program that reads and writes ascii grid files. The DEM and 8 other grids holding the mean and standard deviations of each habitat type surrounding each cell in the model are input to the model. As described above, the mean and standard deviation grids are used to classify the DEM as wetland habitat types. The study area is divided into 3 separate grids to reduce computation time and computer memory requirements. Habitat classified DEM grids are output every ten years of the model run, and a summary file of habitat hectares is provided. For each area, the model was run to simulate 90 years. Output grids were imported into ArcMap software for map making.

Model Results

The 90-year model projections show an overall decrease in wetland habitat area for the northern section, but increases in the central and southern sections (Figures 8, 9, and 10). For all three sections combined, the model predicts there will be little or no net change in wetland habitat area. High marshes and high flats steadily increase during the projection period and offset losses in low marshes and low flats. There is an initial loss of low marsh habitat for 20 to 30 years, stabilization for about 40 years and then a gradual increase in low marsh during the last 20 to 30 years of the projection period. Maps of the model projections are provided in the appendix. The maps show the pattern of upland migration of wetlands and the development of open-water areas.

A.
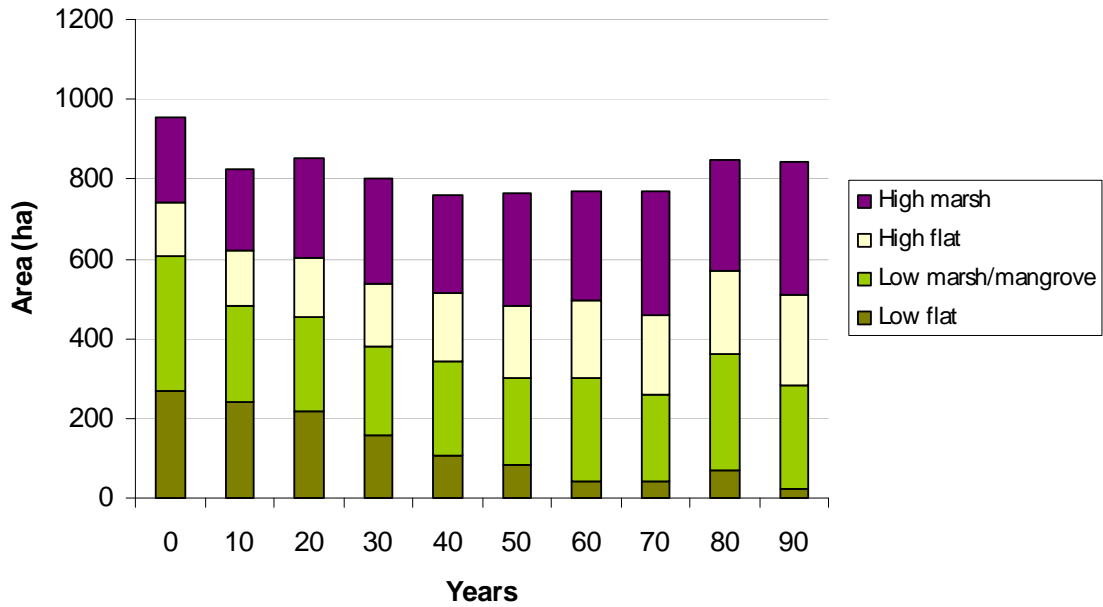
B.
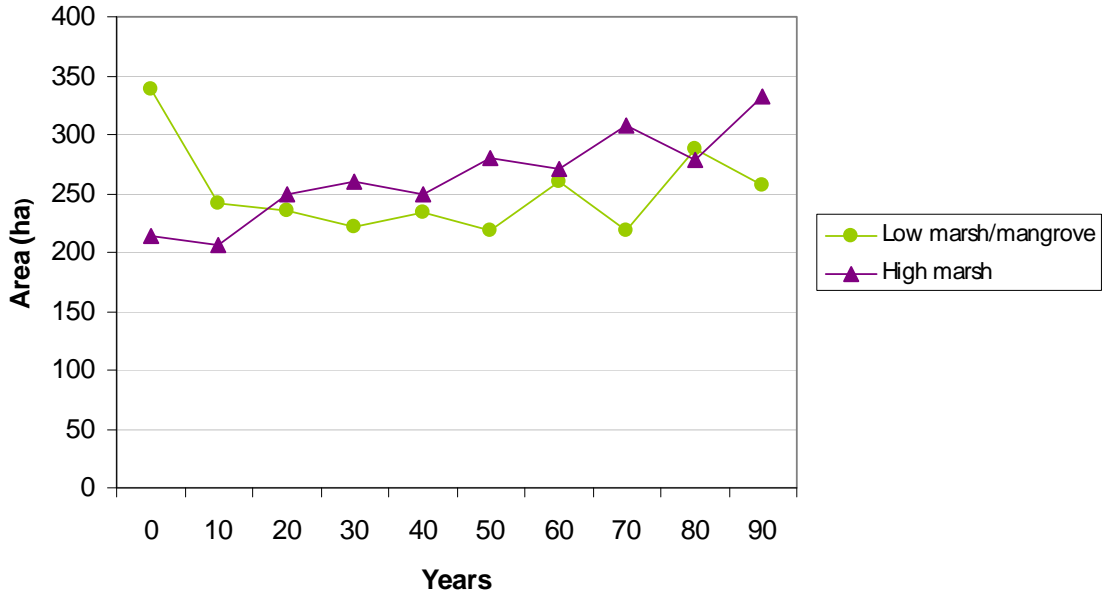
Figure 8. Northern section model-projected habitat change for 90 years at 10-year intervals. See Figure 1 for location of sections. A- All habitat types. B- Comparison of low- and high-marsh habitats.

A.
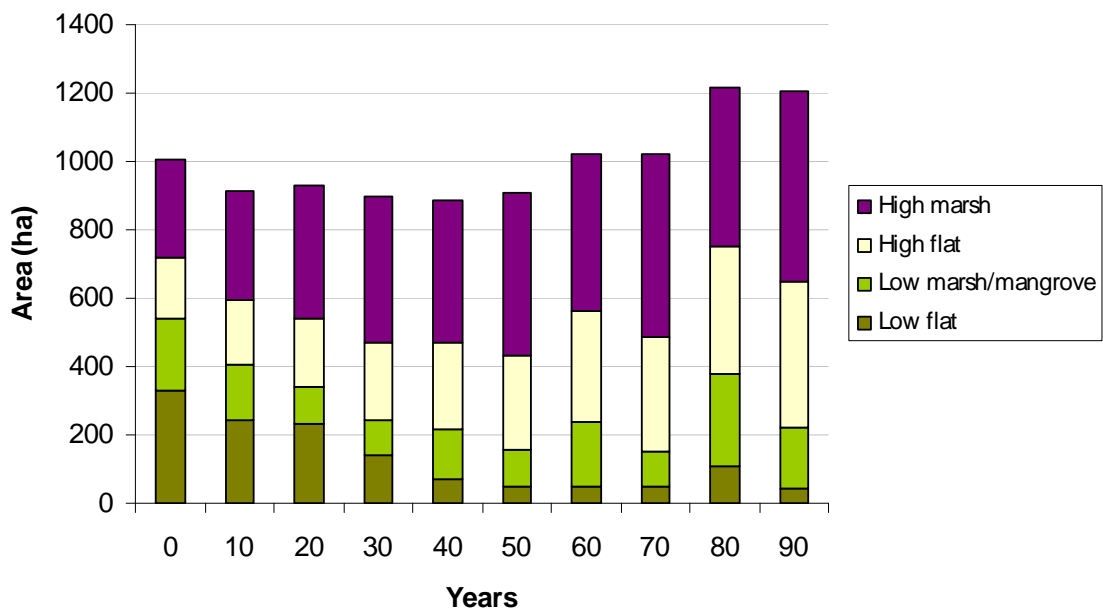
B.
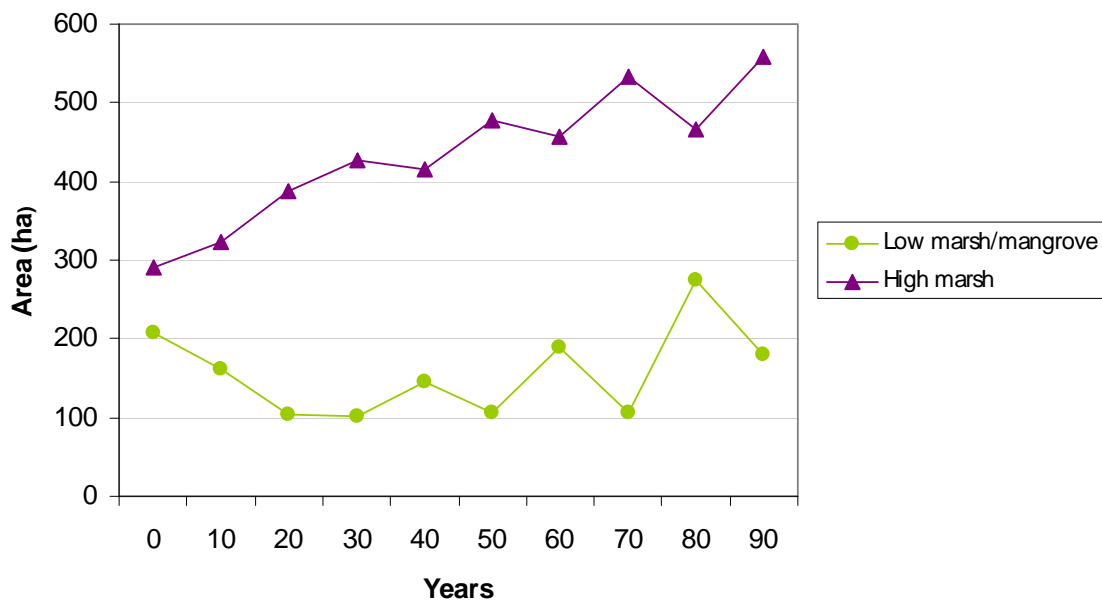
Figure 9. Central section model-projected habitat change for 90 years at 10-year intervals. See Figure 1 for location of sections. A- All habitat types. B- Comparison of low- and high-marsh habitats.

A.

B.
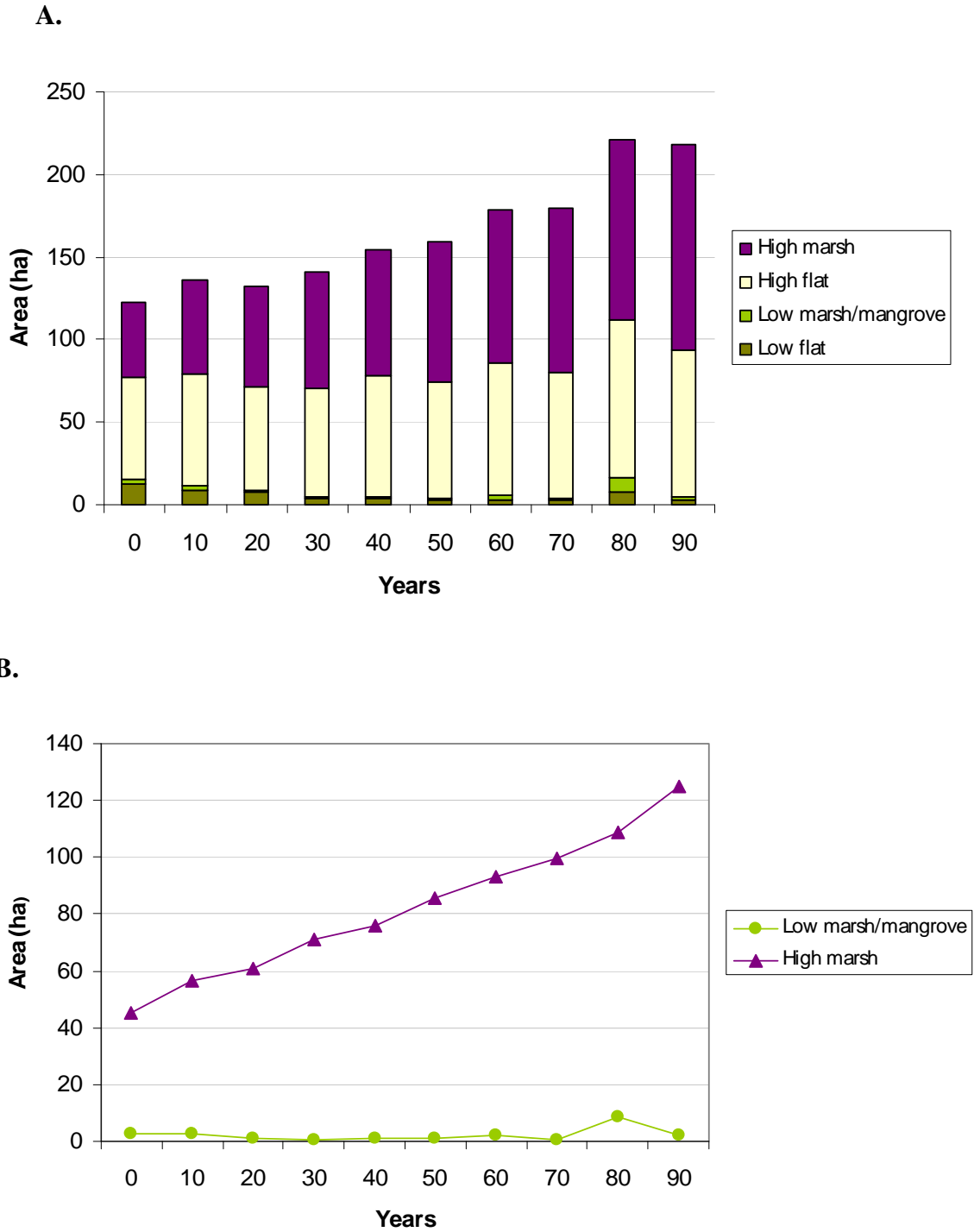
Figure 10. Southern section model-projected habitat change for 90 years at 10-year intervals. See Figure 1 for location of sections. A- All habitat types. B- Comparison of low- and high-marsh habitats.

Discussion

The habitat transition model predicts a slight gain in wetland area over the 90-year modeling period even though relative sea-level rise rates are about twice the global rate. However, there is a shift in the type of wetland with the loss of low marsh and gain of high marsh. The low marsh habitat is inundated daily making it an important habitat in the life cycles of many bay and marine species (e.g., shrimp). The model underestimates the amount of projected low-marsh loss because edge erosion effects are not explicitly included in the model. On the other hand, washover deposition will occur through the established storm washover channels at New Pass and Corpus Christi Pass creating substrate for new wetland development as has happened in the past. These washover processes are not included in the model. Furthermore, the upland migration of wetland habitats, which offsets losses, will only occur if space is preserved for this to happen. The model map results (Appendix) show the areas with the greatest potential for becoming wetland habitat as sea level rises and areas that are most likely to lose wetlands. This information can be used for planning future development and restoration strategies.

References Cited

Allen, J.R.L., 1990, Salt-marsh growth and stratification: A numerical model with special reference to the Severn Estuary, southwest Britain: Marine Geology, v. 95, p. 77-96.

Brinson, M.M., Christian, R.R., and Blum, L.K., 1995, Multiple states in the sea-level induced transition from terrestrial forest to estuary: Estuaries, v. 18, p. 648-659.

Callaway, J.C., DeLaune, R.D., and Patrick, J., W. H., 1997, Sediment accretion rates from four coastal wetlands along the Gulf of Mexico: Journal of Coastal Research, v. 13, p. 181-191.

Callaway, J.C., Nyman, J.A., and DelLaune, R.D., 1996, Sediment accretion in coastal wetlands: A review and a simulation model of processes: Current Topics in Wetland Biogeochemistry, v. 2, p. 2-23.

Cowardin, L.M., Carter, V., Golet, F.C., and LaRoe, E.T., 1979, Classification of wetlands and deepwater habitats of the United States: Washington, D.C., U.S.A., U.S. Department of Interior, Fish and Wildlife Service, p. 131.

Gibeaut, J.C., White, W.A., Smyth, R.C., Andrews, J.R., Tremblay, T.A., Gutiérrez, R., Hepner, T.L., and Neuenschwander, A., 2003, Topographic variation of barrier island subenvironments and associated habitats, Coastal Sediments '03: Crossing disciplinary boundaries: Proceedings, Fifth International Symposium on Coastal Engineering and Science of Coastal Sediment Processes, Volume CD-ROM: Clearwater Beach, Florida, p. 10.

IPCC, 2001, Climate Change 2001: Synthesis Report, Intergovernmental Panel on Climate Change, p. 397.

Krone, R.B., 1987, A method for simulating historic marsh elevations, *in* Kraus, N.C., ed., Coastal Sediments '87, Volume 1: New Orleans, Louisiana, American Society of Civil Engineers, p. 316-323.

Temmerman, S., Govers, G., Meire, P., and Wartel, S., 2003, Modelling long-term tidal marsh growth under changing tidal conditions and suspended sediment concentrations, Scheldt estuary, Belgium: Marine Geology, v. 193, p. 151-169.

White, W.A., Tremblay, T.A., Waldinger, R.L., and Calnan, T.R., 2006, Status and Trends of Wetland and Aquatic habitats on Texas Barrier Islands Coastal Bend: Austin, Bureau of Economic Geology, Jackson School of Geosciences, The University of Texas at Austin, p. 64.

Zervas, C., 2001, Sea Level Variations of the United States 1854-1999, NOAA, National Oceanographic and Atmospheric Administration, p. 66.

Appendix

Corpus Christi Ship Channel

Port Aransas

Gulf of Mexico

Corpus Christi Bay

Northern section - Year 0
Scale 1:60,000

N

Water	
Low marsh/mangrove	
High marsh	
Low flat	
High flat	
Upland	
Buildings/tall vegetation	

0   0.5   1   2   3
Kilometers

Corpus Christi Ship Channel

Port Aransas

Gulf of Mexico

Corpus Christi Bay

Northern section - Year 10
Scale 1:60,000

Water	(light blue)
Low marsh/mangrove	(green)
High marsh	(purple)
Low flat	(dark olive)
High flat	(tan)
Upland	(brown)
Buildings/tall vegetation	(gray)

N

0   0.5   1   2   3
Kilometers

Corpus Christi Ship Channel

Port Aransas

Gulf of Mexico

Corpus Christi Bay

Northern section - Year 20
Scale 1:60,000

Water
Low marsh/mangrove
High marsh
Low flat
High flat
Upland
Buildings/tall vegetation

| 0 | 0.5 | 1 | 2 | 3 |
Kilometers

Corpus Christi Ship Channel

Port Aransas

Gulf of Mexico

Corpus Christi Bay

Northern section - Year 30
Scale 1:60,000

Water	
Low marsh/mangrove	
High marsh	
Low flat	
High flat	
Upland	
Buildings/tall vegetation	

0   0.5   1   2   3
Kilometers

Corpus Christi Ship Channel

Port Aransas

Gulf of Mexico

Corpus Christi Bay

Northern section - Year 40
Scale 1:60,000

N

Water	
Low marsh/mangrove	
High marsh	
Low flat	
High flat	
Upland	
Buildings/tall vegetation	

0   0.5   1   2   3
Kilometers

Corpus Christi Ship Channel

Port Aransas

Gulf of Mexico

Corpus Christi Bay

Northern section - Year 50
Scale 1:60,000

N

Water	
Low marsh/mangrove	
High marsh	
Low flat	
High flat	
Upland	
Buildings/tall vegetation	

0   0.5   1   2   3
Kilometers

Corpus Christi Ship Channel

Port Aransas

Gulf of Mexico

Corpus Christi Bay

Northern section - Year 60
Scale 1:60,000

N

Water	
Low marsh/mangrove	
High marsh	
Low flat	
High flat	
Upland	
Buildings/tall vegetation	

0   0.5   1   2   3
Kilometers

Corpus Christi Ship Channel

Port Aransas

Gulf of Mexico

Corpus Christi Bay

Northern section - Year 70
Scale 1:60,000

Water
Low marsh/mangrove
High marsh
Low flat
High flat
Upland
Buildings/tall vegetation

0   0.5   1   2   3
Kilometers

Corpus Christi Ship Channel

Port Aransas

Gulf of Mexico

Corpus Christi Bay

Northern section - Year 80
Scale 1:60,000

N

Color	Legend
Water	Water
Low marsh/mangrove	Low marsh/mangrove
High marsh	High marsh
Low flat	Low flat
High flat	High flat
Upland	Upland
Buildings/tall vegetation	Buildings/tall vegetation

0   0.5   1   2   3
                              Kilometers

Corpus Christi Ship Channel

Port Aransas

Gulf of Mexico

Corpus Christi Bay

Northern section - Year 90
Scale 1:60,000

N

Water
Low marsh/mangrove
High marsh
Low flat
High flat
Upland
Buildings/tall vegetation

0   0.5   1   2   3
Kilometers

Corpus Christi Bay

Gulf of Mexico

Fish Pass

Central section - Year 0

Scale 1:60,000

Water
Low marsh/mangrove
High marsh
Low flat
High flat
Upland
Buildings/tall vegetation

N

0   0.5   1   2   3
Kilometers

Packery Channel

33

Corpus Christi Bay

Gulf of Mexico

Fish Pass

Packery Channel

Central section - Year 10

Scale 1:60,000

Water

Low marsh/mangrove

High marsh

Low flat

High flat

Upland

Buildings/tall vegetation

0   0.5   1   2   3

Kilometers

Corpus Christi Bay

Gulf of Mexico

Fish Pass

Central section - Year 20
Scale 1:60,000

Water
Low marsh/mangrove
High marsh
Low flat
High flat
Upland
Buildings/tall vegetation

N

0   0.5   1   2   3
Kilometers

Packery Channel

Corpus Christi Bay

Gulf of Mexico

Fish Pass

Packery Channel

Central section - Year 30
Scale 1:60,000

N

	Water
	Low marsh/mangrove
	High marsh
	Low flat
	High flat
	Upland
	Buildings/tall vegetation

0   0.5   1   2   3
Kilometers

Corpus Christi Bay

Gulf of Mexico

Fish Pass

Central section - Year 40
Scale 1:60,000

Water
Low marsh/mangrove
High marsh
Low flat
High flat
Upland
Buildings/tall vegetation

0   0.5   1   2   3
                              Kilometers

Packery Channel

Corpus Christi Bay

Gulf of Mexico

Fish Pass

Central section - Year 50
Scale 1:60,000

	Water
	Low marsh/mangrove
	High marsh
	Low flat
	High flat
	Upland
	Buildings/tall vegetation

0   0.5   1   2   3
Kilometers

Packery Channel

Corpus Christi Bay

Gulf of Mexico

Fish Pass

Packery Channel

Central section - Year 60
Scale 1:60,000

Water
Low marsh/mangrove
High marsh
Low flat
High flat
Upland
Buildings/tall vegetation

0   0.5   1   2   3
                        Kilometers

Corpus Christi Bay

Gulf of Mexico

Fish Pass

Central section - Year 70

Scale 1:60,000

Water

Low marsh/mangrove

High marsh

Low flat

High flat

Upland

Buildings/tall vegetation

| 0 | 0.5 | 1 | | 2 | | 3 | |
Kilometers

Packery Channel

Corpus Christi Bay

Gulf of Mexico

Fish Pass

Central section - Year 80
Scale 1:60,000

Water
Low marsh/mangrove
High marsh
Low flat
High flat
Upland
Buildings/tall vegetation

0   0.5   1   2   3
Kilometers

Packery Channel

41

Corpus Christi Bay

Gulf of Mexico

Fish Pass

Central section - Year 90
Scale 1:60,000

Water
Low marsh/mangrove
High marsh
Low flat
High flat
Upland
Buildings/tall vegetation

0   0.5   1   2   3
Kilometers

Packery Channel

Packery Channel

Gulf of Mexico

Gulf Intracoastal Waterway

Southern section - Year 0
Scale 1:60,000

N

	Water
	Low marsh/mangrove
	High marsh
	Low flat
	High flat
	Upland
	Buildings/tall vegetation

0   0.5   1   2   3
Kilometers

Packery Channel

Gulf of Mexico

Gulf Intracoastal Waterway

Southern section - Year 10
Scale 1:60,000

N

	Water
	Low marsh/mangrove
	High marsh
	Low flat
	High flat
	Upland
	Buildings/tall vegetation

0   0.5   1   2   3
Kilometers

Packery Channel

Gulf Intracoastal Waterway

Gulf of Mexico

Southern section - Year 20
Scale 1:60,000

Water
Low marsh/mangrove
High marsh
Low flat
High flat
Upland
Buildings/tall vegetation

0   0.5   1   2   3
Kilometers

Packery Channel

Gulf of Mexico

Gulf Intracoastal Waterway

Southern section - Year 30
Scale 1:60,000

Water
Low marsh/mangrove
High marsh
Low flat
High flat
Upland
Buildings/tall vegetation

0   0.5   1   2   3
Kilometers

Packery Channel

Gulf of Mexico

Gulf Intracoastal Waterway

Southern section - Year 40
Scale 1:60,000

	Water
	Low marsh/mangrove
	High marsh
	Low flat
	High flat
	Upland
	Buildings/tall vegetation

0   0.5   1   2   3
Kilometers

Packery Channel

Gulf Intracoastal Waterway

Gulf of Mexico

Southern section - Year 50
Scale 1:60,000

Water	
Low marsh/mangrove	
High marsh	
Low flat	
High flat	
Upland	
Buildings/tall vegetation	

N

0   0.5   1   2   3
Kilometers

Packery Channel

Gulf of Mexico

Gulf Intracoastal Waterway

Southern section - Year 60
Scale 1:60,000

	Water
	Low marsh/mangrove
	High marsh
	Low flat
	High flat
	Upland
	Buildings/tall vegetation

N

0   0.5   1   2   3
Kilometers

Packery Channel

Gulf of Mexico

Gulf Intracoastal Waterway

Southern section - Year 70
Scale 1:60,000

Water
Low marsh/mangrove
High marsh
Low flat
High flat
Upland
Buildings/tall vegetation

N

| 0 | 0.5 | 1 | 2 | 3 |
Kilometers

Packery Channel

Gulf of Mexico

Gulf Intracoastal Waterway

Southern section - Year 80
Scale 1:60,000

	Water
	Low marsh/mangrove
	High marsh
	Low flat
	High flat
	Upland
	Buildings/tall vegetation

0   0.5   1   2   3
Kilometers

Packery Channel

Gulf of Mexico

Gulf Intracoastal Waterway

Southern section - Year 90

Scale 1:60,000

N

	Water
	Low marsh/mangrove
	High marsh
	Low flat
	High flat
	Upland
	Buildings/tall vegetation

0   0.5   1   2   3
Kilometers